Time-Resolved Spectroscopic Studies of B_{12} Coenzymes: Comparison of the Influence of Solvent on the Primary Photolysis Mechanism and Geminate Recombination of Methyl-, Ethyl-, *n*-Propyl-, and 5′-Deoxyadenosylcobalamin

Roseanne J. Sension,* D. Ahmasi Harris, and Allwyn G. Cole

Departments of Chemistry and Physics, University of Michigan, Ann Arbor, Michigan 48109-1055

Received: June 14, 2005; In Final Form: September 12, 2005

A transient absorption study of the photolysis of methylcobalamin (MeCbl), ethylcobalamin (EtCbl), and *n*-propylcobalamin (PrCbl) in ethylene glycol spanning six decades in time, from 10 fs to 10 ns, is reported. These measurements probe the influence of solvent on the formation and decay of the metal-to-ligand charge transfer (MLCT) intermediate observed following excitation of MeCbl, the photolysis mechanism in EtCbl and PrCbl, and the rate constants for geminate recombination of the alkyl radicals with cob(II)alamin and for the escape of the alkyl radicals from the initial solvent cage. Earlier investigations probed the dynamics of 5′-dexoyadenosylcobalamin (coenzyme B_{12}) in water and ethylene glycol (Yoder, L. M.; Cole, A. G.; Walker, L. A., II; Sension, R. J. *J. Phys. Chem. B* **2001**, *105*, 12180−12188) and alkylcobalamins in water (Cole, A. G.; Yoder, L. M.; Shiang, J. J.; Anderson, N. A.; Walker, L. A., II; Banaszak Holl, M. M.; Sension, R. J. *J. Am. Chem. Soc.* **2002**, *124*, 434−441). The results of these investigations are discussed in the context of the literature on the frictional influence of solvent on chemical reaction dynamics. The measurements allow a separation of the influence of the solvent on the intrinsic rate constant for geminate recombination and the rate constant for escape from the initial solvent cage. The rate constant for the intrinsic geminate recombination of cob(II)alamin with the alkyl radical is weakly dependent on the solvent and on the nature of the alkyl radical (Me, Et, Pr, or Ado). The Et, Pr, and Ado radicals exhibit the behavior expected for diffusion-controlled escape from the initial solvent cage. In contrast, the magnitude of cage escape for the Me radical is much larger than anticipated on the basis of hydrodynamic arguments.

Introduction

The B_{12}-dependent enzymes may be divided into two broad categories, methyltransferase enzymes and mutase enzymes, distinguished by the identity of the specific form of the B_{12} coenzyme involved (see Figure 1).[1−5] In the methyltransferase enzymes, methylcobalamin (MeCbl), or a closely related methylcorrinoid, acts as a methyl donor. These enzymes function through heterolytic cleavage of the cobalt−carbon bond to form cob(I)alamin, with the methyl group formally transferred as a methyl cation. Thus, the cobalt cycles between Co(I) and Co(III) states.[6,7] The most extensively characterized methyltransferase enzyme is methionine synthase, although several other methylcorrinoid dependent enzymes have been reported.[8−10] In contrast, adenosylcobalamin-dependent (coenzyme B_{12}, AdoCbl) mutase enzymes catalyze rearrangement reactions that proceed via mechanisms involving organic radicals generated by homolysis of the coenzyme cobalt−carbon bond to produce an adenosyl radical and cob(II)alamin.[1,7] Although B_{12}-dependent enzymes are mainly confined to microbial organisms, both AdoCbl-dependent methylmalonyl-CoA mutase and MeCbl-dependent methionine synthase are essential enzymes in animals, including humans.

Despite extensive experimental effort[7,11] and, more recently, density functional (DFT) calculations,[12−23] it is not yet clear how carbon−cobalt bond reactivity can be directed so differently in the methyl- and adenosylcobalamin coenzymes. In particular, is the cleavage pattern a result of the influence of the enzymatic environment on axial bond lengths or on the relative stability of the cob(II)alamin or cob(I)alamin product, or alternatively,

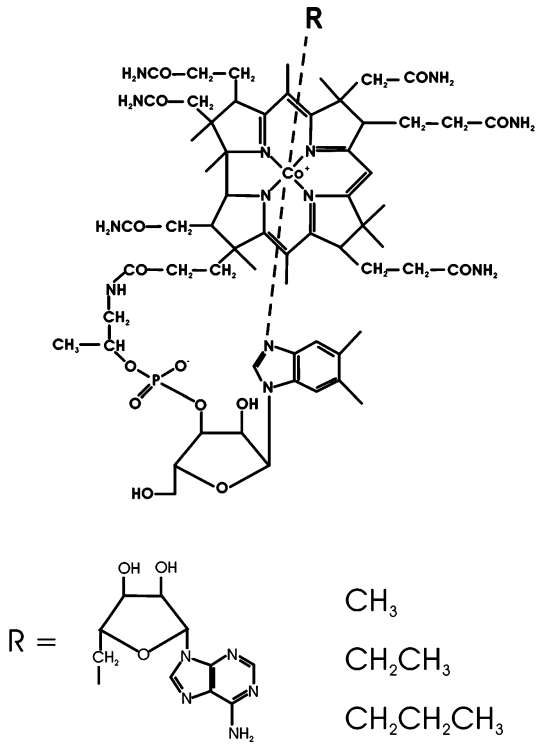

Figure 1. Schematic diagram of alkylcobalamins.

* Corresponding author. E-mail: rsension@umich.edu.

10.1021/jp053202w CCC: $30.25 © 2005 American Chemical Society
Published on Web 10/25/2005

is it an intrinsic property of the alkylcobalamin, largely independent of the environment? Although this is still an open question, many experimental and theoretical investigations are predicated on the assumption that alkyl ligands are interchangeable. In addition, all of the DFT investigations and many of the experimental studies ignore or restrict the influence of solvent or protein environment on the electronic structure and reactivity of the Co−C bond.

In recent studies we have investigated the influence of environment on the electronic spectrum and photochemistry of AdoCbl.[24−28] The photochemistry of adenosylcobalamin (AdoCbl) is found to be inherently dependent upon its environment. Excitation of AdoCbl bound to glutamate mutase results in formation of a MLCT (metal−ligand charge transfer) intermediate state, which decays with a 105 ps time constant to form cob(II)alamin.[28] This is in contrast to our earlier measurements of AdoCbl dissolved in water, where the photohomolysis proceeds through an intermediate state with a spectrum characteristic of the dissociation of the axial dimethylbenzimidazole (DMB) ligand,[25−27] and measurements in ethylene glycol where rapid formation of a cob(II)alamin-like difference spectrum is observed.[27] The differences observed in the photodissociation pathway as a function of solvent do not correlate with changes in the linear absorption spectra but rather may reflect changes in the relative energies of the relaxed electronic states.

Because the macroscopic dielectric properties of the environment and the microscopic hydrogen-bonding interactions of the surroundings (ethylene glycol, water, or protein) may influence both the photolysis and thermolysis of cobalamins, it is useful to explore the influence of solvent on the photolysis and geminate recombination of alkylcobalamins. In this paper we extend our studies to explore the effect of the solvent environment, ethylene glycol vs water, on the photolysis of MeCbl, ethylcobalamin (EtCbl), and *n*-propylcobalamin (PrCbl) and compare these results with those reported earlier for AdoCbl.[27] These comparisons provide additional insights into the photolysis mechanism in both solvents and on the influence of alkyl ligand and solvent environment on the inherent reactivity of the Co−C bond. In particular, influence of solvent on the branching between the cob(III)alamin MLCT state and prompt bond homolysis may shed light on the nature of the observed electronic state. There are several reasons for the choice of ethylene glycol as a solvent for comparison. Ethylene glycol is a more viscous solvent with a higher boiling point than water. In addition, the static dielectric constant of ethylene glycol is approximately half that of liquid water (37 vs 78.5 at 25 °C),[29] providing a more proteinlike environment.

An additional motivation for the study of photolysis and geminate recombination in alkylcobalamins as a function of solvent is the evaluation of the various factors involved in geminate recombination and escape from a solvent cage. The influence of the cage effect on geminate recombination was brought to prominence by Noyes in the 1950s[30−34] and has been investigated extensively, both theoretically and experimentally in the ensuing years. The quantum yield for geminate recombination in a viscous medium is limited by the ability of the radicals formed in a bond homolysis reaction to diffuse away from each other. Thus, the quantum yield represents a competition between the rate of recombination and the rate of escape from the solvent cage.

The influence of cage recombination on the homolysis of organometallic bonds in general, and alkylcobalamins in particular, was initially put forth by Koenig and Finke as important in the experimental determination of the bond dissociation energy of MeCbl and AdoCbl.[35,36] A subsequent investigation of the effect of viscosity on thermal and photolytic homolysis of AdoCbl was reported by Gerards et al.[37] In this paper the viscosity dependence of the photoinduced and thermal homolysis of AdoCbl in the presence of a radical trap was analyzed to extract a caging fraction. However, analysis of thermal homolysis and continuous wave photolysis measurements suffer from the necessity of assumptions about the primary steps, which may or may not be valid. In principle, time-resolved spectroscopic measurements allow the direct monitoring of intermediates in real time, requiring fewer assumptions and permitting a direct test of some of the commonly made assumptions. Early time-resolved experiments placed some limits on geminate recombination but suffered from errors and uncertainties introduced by the inherent noise of the measurements, by assumptions made in the interpretation of the data, or by the limited spectral range available in the measurement.[38−41] The time-resolved spectral measurements of the alkylcobalamins reported here permit the determination of the rate constants for both geminate recombination and for escape from the initial solvent cage as a function of the size of the alkyl radical and the viscosity of the solvent. These studies open a door for a thorough investigation of the dynamics of cage escape and radical recombination in a complex and intrinsically interesting model system.

Experimental Methods

Transient Absorption Measurements. Transient absorption measurements were performed using a femtosecond laser system and experimental method as described previously.[27,42] Briefly, a self-mode-locked titanium sapphire oscillator, running at 80 MHz and producing 20 fs and 2 nJ pulses, was amplified at a 1 kHz repetition rate in a regenerative amplifier or in a multipass amplifier. The resulting laser beam was centered at approximately 800 nm, providing 400 μJ and 70 fs pulses at a repetition rate of 1 kHz. Tunable probe pulses were generated by sending the 800 nm laser pulse into a home-built optical parametric amplifier constructed according to the design of Riedle and co-workers.[43] For the present set of measurements the output consisted of 100−200 fs pulses centered at peak wavelengths between 470 and 633 nm inclusive. At each wavelength a 10 nm band-pass interference filter was used to limit the spectral bandwidth of the probe pulse. For kinetic measurements the probe pulses were delayed with respect to the pump pulses by a 1.5 m computer-controlled motorized translation stage (Newport-Klinger). This stage allows measurements to be made with femtosecond resolution (1 μm step size = 6.7 fs of delay) out to a maximum time delay of ca. 10 ns. Traces were collected from −10 to 9 ns using variable time steps, typically 0.1 ps (−10 to −1 ps), 0.025 ps (−1 to 1 ps), 0.050 ps (1−5 ps), 0.1 ps (5−10 ps), 0.2 ps (10−20 ps), 0.5 ps (20−50 ps), 1 ps (50−100 ps), 2 ps (100−200 ps), 5 ps (200−500 ps), 10 ps (500 ps−1 ns), 20 ps (1−2 ns), and 50 ps (2−9 ns). Broad-band spectral measurements at selected time delays were made by using a white light continuum probe and a spectrometer for analysis as described previously.[26,44] For all of the measurements reported here the excitation wavelength was 400 nm produced by generating the second harmonic of the Ti:Sapphire laser. The cross-correlation of the pump and probe pulses was as long as 450 fs with a 470 nm probe but more typically fell between 250 and 350 fs.

Sample Preparation. Synthesis and purification of EtCbl and PrCbl were carried out according to literature methods as described in our previous paper.[42] MeCbl was purchased from

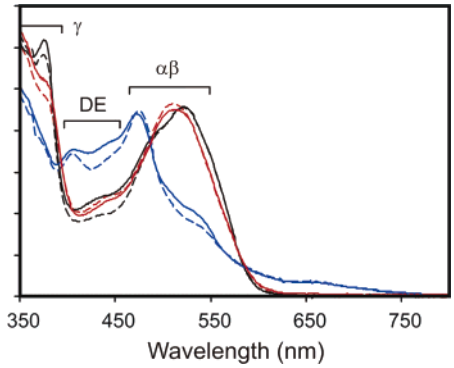

Figure 2. Absorption spectra of methylcobalamin (black), *n*-propylcobalamin (red), and cob(II)alamin (blue). The dashed lines are the spectra in water, and the solid lines, spectra in ethylene glycol. The traditional nomenclature for the spectral regions designated in cobalamins $\alpha\beta$, DE, and γ are also indicated.

Sigma and used as received. The ethylene glycol solvent was deoxygenated by freeze−pump−thaw techniques and maintained under nitrogen until use. After addition of alkylcobalamin and during measurements a positive-pressure argon atmosphere was used to prevent contamination with oxygen. Samples were prepared with alkylcobalamin concentrations of ca. 2 mM. The solutions were flowed through a 1 mm path-length cell with a rate sufficient to refresh the illuminated volume between laser pulses. UV−visible spectra of the samples obtained before and after laser exposure were identical, indicating minimal photoproduct accumulation during the course of an experiment.

Steady-State Spectral Measurements. Absorption spectra of MeCbl, EtCbl, and PrCbl in deoxygenated ethylene glycol were obtained using a dual beam UV−vis spectrophotometer. A spectrum of cob(II)alamin in ethylene glycol was generated by CW photolysis from MeCbl using a tungsten lamp as described previously.[44] A 40 μM solution of MeCbl was prepared in deoxygenated ethylene glycol, in the presence of 1 mM TEMPO as a radical scavenger. The sample was handled in the dark at all times prior to measurement, and an oxygen-free environment was maintained. The cob(II)alamin species was produced by illuminating the sample for 2 min intervals until no further change in the absorption spectrum was observed. Generation of cob(II)alamin in this manner permits construction of an absolute difference spectrum for comparison with time-resolved measurements. An absolute difference spectrum was also obtained for PrCbl in ethylene glycol, although the reactivity of the *n*-propyl radical made it difficult to drive the reaction to completion in this case. In ethylene glycol, as in water, the visible absorption spectra of EtCbl and PrCbl are indistinguishable.[42]

Results

Steady-State Absorption Spectra. The UV−visible absorption spectra of cobalamins are characteristic of oxidation state, axial ligation, and environment. The absorption spectra of MeCbl, PrCbl, and cob(II)alamin obtained in water and ethylene glycol are shown in Figure 2. To quantify the spectral changes that are observed when moving from MeCbl to EtCbl or PrCbl, a least-squares Gaussian peak fit was performed for each cob(III)alamin absorption spectrum. The results of this fit as a function of solvent are shown in Figure 3. At least four Gaussian bands are required to model the visible absorption spectrum.

The lowest two bands, or $\alpha\beta$-bands in alkylcobalamins and other cob(III)alamins, are generally assigned as vibronic bands of the HOMO−LUMO transition. Resonance Raman spectra

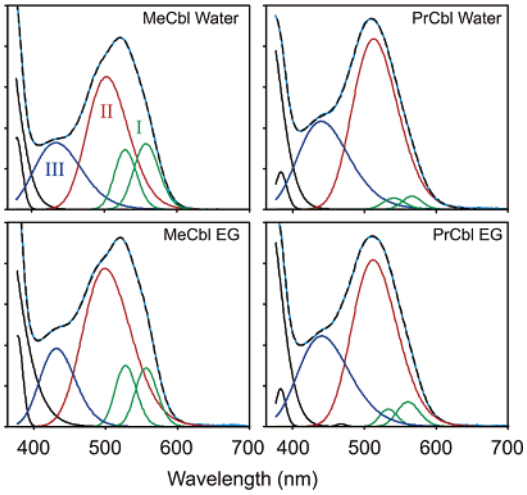

Figure 3. Gaussian decomposition of the visible absorption spectrum of MeCbl and PrCbl in water and ethylene glycol.

of cobalamin compounds exhibit enhancement of vibrations in the 1000−1500 cm^{-1} region consistent with a vibronic assignment for these transitions.[19,20,45−50] Nevertheless, this assignment is not entirely secure. The corrin ring without cobalt has a visible absorption spectrum similar to that observed for cob(III)alamins and exhibits a fluorescence spectrum at room temperature and at low temperature with two distinct bands.[51,52] However, Fugate et al. report that the relative intensities of these fluorescence bands are dependent upon cooling conditions suggesting that they correspond to different conformers or tautomers. Higher vibronic transitions are not observed in the fluorescence despite the fact that the α and β bands in the absorption spectrum are of comparable intensity. Thus, the mirror image vibronic structure is missing from the fluorescence spectrum, suggesting that the $\alpha\beta$ bands, at least in the metal-free corrin, are not vibronic transitions.

An additional transition, accounting for much of the oscillator strength, lies on the high-energy side of the $\alpha\beta$ band. Brunold and co-workers have performed a series of low-temperature CD and MCD measurements of MeCbl and other cob(III)alamins.[19] For MeCbl a sign change in the CD spectrum suggests a different electronic origin for band II (ref 19, Figure S2 in Supporting Information). Likewise, the visible transition peaking around 23 000 cm^{-1} (band III) correlates with a change in sign in the CD spectrum. Thus, the visible absorption spectrum contains contributions from at least three distinct electronic transitions.

The principal differences between the visible absorption spectra of the alkylcobalamins under investigation here lie in this $\alpha\beta$-band region. The $\alpha\beta$-bands are much less prominent in the absorption spectra of EtCbl and PrCbl than in MeCbl or AdoCbl. The Gaussian peak fit shown in Figure 3 suggests that the blue shift of the EtCbl and PrCbl absorption spectra relative to the spectra of MeCbl and AdoCbl (see Figure 2) is due to a change in the relative oscillator strengths of the $\alpha\beta$-band and band II. Alternatively, the data may be consistent with a blue shift of the $\alpha\beta$-band transitions under the band II transition.

Additional insight into the electronic structure of cobalamins may be obtained from theoretical calculations. A number of time-dependent density functional (TD-DFT) calculations of the electronic structure and electronic spectrum of cobalamins have appeared in the literature recently.[12,18−20,22,53] Most of these papers report calculations for cyanocobalamin (vitamin B_{12}, CNCbl) models. However, Brunold and co-workers report calculations on models of MeCbl and other cob(III)alamins.[19]

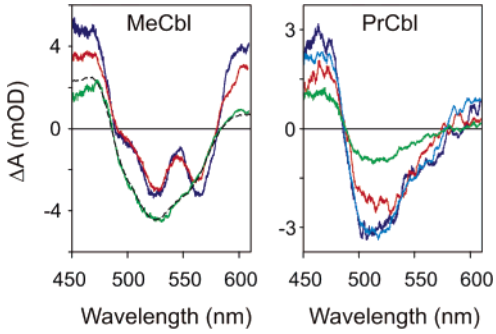

Figure 4. Visible difference spectra observed following the excitation of MeCbl and PrCbl at 400 nm. The spectra were obtained for time delays of the following: (dark blue) 60 ps MeCbl, 40 ps PrCbl; (light blue) 100 ps; (red) 1 ns; (green) 7 ns MeCbl, 5 ns PrCbl. The dashed black line is the steady-state difference spectrum for the formation of cob(II)alamin from MeCbl.

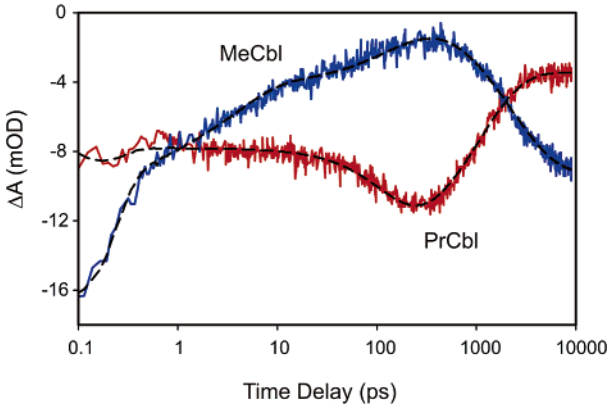

Figure 5. Sample kinetic traces. These traces were obtained at 540 nm for MeCbl (blue) and PrCbl (red) in ethylene glycol. The picosecond component is hard to pick out at this wavelength, but the subpicosecond components, 100−200 ps components, and the nanosecond decays are clearly required to fit the data.

The consensus of the DFT calculations is similar to that reported in earlier semiempirical calculations.[54] In particular, the DFT calculations of the absorption spectra of MeCbl, aquocobalamin (H_2OCbl), and CNCbl do an excellent job in the near UV, reproducing many of the trends observed in the γ-band region.[19]

In the visible region of the spectrum, the DFT calculations report three bands of approximately equal intensity. These three bands may be tentatively assigned to the three bands observed in the Gaussian decomposition. The lowest energy transition is the HOMO → LUMO transition, predominantly a $\pi \rightarrow \pi^*$ transition of the corrin ring. However, the calculated differences in the visible spectra of MeCbl, H_2OCbl, and CNCbl are much larger than the differences in the actual experimental spectra. The discrepancies in the visible region of the spectrum may reflect the intrinsic difficulty that TD-DFT has with states possessing charge-transfer character. Thus, the calculations have qualitative but not yet quantitative value in interpreting the observed spectra and describing the electronic structure.

Transient Absorption Data. Transient absorption traces for MeCbl, EtCbl, and PrCbl in ethylene glycol were obtained using probe wavelengths of 470, 500, 520, 540, 560, 570 (MeCbl only), 600, and 633 nm. These wavelengths span the visible absorption spectrum from the peak of the cob(II)alamin product spectrum through the remainder of the alkylcobalamin $\alpha\beta$-band absorption. In addition transient absorption spectra were obtained for several pump−probe time delays between 20 ps and 8 ns (Figure 4). For all three of these compounds the gross features of the photochemistry are unchanged from that observed in aqueous solution. The photolysis of MeCbl is characterized by branching between prompt bond homolysis and formation of a cob(III)alamin MLCT excited state as observed in water.[25,42,44] A singular value decomposition analysis (SVD) of the difference spectra of MeCbl yields two independent difference spectra corresponding to cob(II)alamin and the MLCT state. Both EtCbl and PrCbl undergo rapid bond homolysis forming a cob(II)-alamin product on a picosecond time scale.

To separate and analyze the dynamics in the alkylcobalamins, the time-resolved absorption changes measured at seven or eight probe wavelengths spanning the visible absorption spectrum were fitted to a model consisting of a sum of exponential decay components. For each cobalamin compound the data required four exponential components and a component which does not decay during the 9 ns window of the present measurements.

$$S(\lambda) = \sum_{n=1}^{4} a_n e^{-k_n t} + a_p \qquad (1)$$

Typical traces obtained for MeCbl and PrCbl are shown in Figure 5. The fastest rate constant, k_1, reflects the decay of the initially excited state within a hundred femtoseconds of excitation. This decay is faster than the instrument response and is not analyzed in this paper. The remaining three rate constants obtained from these fits are summarized in Table 1.

Photolysis of Ethyl- and *n*-Propylcobalamin. The behavior of EtCbl and PrCbl are identical with each other and with the behavior in aqueous solution. Assuming a model with a stepwise progression through three intermediate states prior to formation of the solvent separated radical pair, the species associated difference spectra shown in Figure 6 are obtained.[27] The difference spectra deduced for all three intermediate states are characterized by a bleach of the visible absorption band, similar to that expected for the formation of cob(II)alamin. This is consistent with the behavior reported earlier for EtCbl and PrCbl in water following excitation at 400 nm.[42] The ca. 2 ps component is of small amplitude and probably reflects vibrational relaxation of the corrin ring rather than a true "intermediate state". This component is required to fit the data at 470, 560, and 600 nm in both water and ethylene glycol but is not required at the other wavelengths.

The 100 ps component in ethylene glycol is characterized by a decrease in absorption in the 500−633 nm range and an increase in absorption at 470 nm. A similar, but much faster, 20 ps evolution of the spectrum is observed in water.[42] The evolution of the spectrum is consistent with relaxation of the corrin ring in the solvent environment. The more viscous ethylene glycol solvent hinders the relaxation. These results suggest the formation of the radical pair on a subpicosecond time scale following excitation at 400 nm. The subsequent dynamics reflect vibrational and conformational relaxation of the cob(II)alamin. However, the possibility that the 100 ps component in ethylene glycol and 20 ps component in water reflect bond homolysis from the lowest excited electronic state cannot be ruled out.

The longest time constant required to model the data (1.2 ns for PrCbl and 0.95 ns for EtCbl) reflects the competition between geminate recombination of the radical pair and escape from the initial solvent cage confining the alkyl radical to the vicinity of the cobalt. Both the solvent environment and the size of the alkyl radical influence the competition between geminate recombination of the radical pair and diffusion of the alkyl radical. In ethylene glycol the quantum yield for formation

TABLE 1: Summary of Rate Constants (and Time Constants) Observed for MeCbl, EtCbl, and PrCbl in Ethylene Glycol

constant	MeCbl[a]	EtCbl[a]	PrCbl[a]	AdoCbl[b]
k_2 (ps^{-1})	0.27 ± 0.01 (3.7 ps)	0.47 ± 0.05 (2.1 ps)	0.49 ± 0.13 (2.0 ps)	
k_3 (ns^{-1})	5.7 ± 0.04 (175 ps)	9.0 ± 1.0 (110 ps)	10.5 ± 1.9 (95 ps)	
k_4 (ns^{-1})	0.41 ± 0.03 (2.4 ns)	1.05 ± 0.08 (0.95 ns)	0.84 ± 0.07 (1.2 ns)	
ϕ (at 9 ns)[c]	0.74 ± 0.05	0.40 ± 0.10	0.29 ± 0.10	0.08 ± 0.02
k_r (ns^{-1})[d]	1.5 ± 0.2	0.68 ± 0.15	0.60 ± 0.15	1.34 ± 0.10
k_{esc} (ns^{-1})[d]	4.2 ± 0.2	0.45 ± 0.15	0.24 ± 0.15	0.11 ± 0.10

[a] Uncertainties in the rate constants k_{2-4} and the quantum yield, ϕ, represent one standard deviation of the distribution of values obtained from fitting the different experimental traces for each cobalamin. [b] Data from ref 27. [c] The quantum yield, ϕ, is determined from the relative amplitudes of the long-lived radical pair and the decay of the cob(II)alamin difference spectrum attributed to geminate recombination as described previously.[27] [d] The rate constants k_r and k_e are calculated from $\phi = k_e/(k_r + k_e)$, where $k_3 = k_r + k_e$ in MeCbl and $k_4 = k_r + k_e$ in EtCbl and PrCbl.

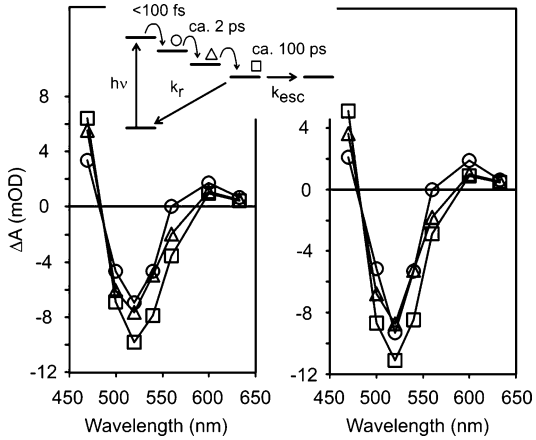

Figure 6. Species-associated difference spectra for EtCbl (left) and PrCbl (right) deduced from the decay-associated difference spectra by assuming a stepwise model for the formation of the solvent-separated radical pair. The circles represent the spectrum of the first clearly identifiable intermediate state formed on a time scale <100 fs. Evolution on the picosecond time scale leads to the formation of the long-lived cob(II)alamin spectrum (squares).

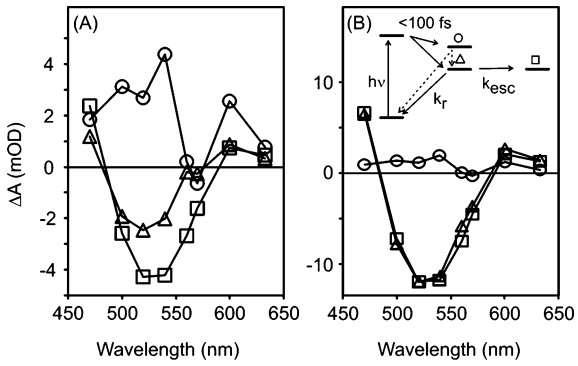

Figure 7. (A) Decay-associated difference spectra obtained from the fit of the transient absorption data obtained for MeCbl in ethylene glycol: triangles, $k_3 = 5.7$ ns^{-1}; circles, $k_4 = 0.41$ ns^{-1}; squares, $k \ll 0.1$ (nondecaying component). (B) Species-associated spectra corresponding to the MLCT excited state (circles), the geminate radical pair (triangles), and the solvent-separated radical pair (squares).

of a long-lived radical pair is 0.40 ± 0.10 for EtCbl and 0.29 ± 0.10 for PrCbl.

Photolysis of Methylcobalamin. The spectral changes observed for MeCbl suggest a different model for the initial photochemistry. The decay-associated spectra for MeCbl are shown in Figure 7A. The data are similar to that obtained for MeCbl in water.[25,42] The increased viscosity of the ethylene glycol solvent compared with water influences the dynamics in two ways. First, the decay of the MLCT excited state is significantly slower, 2.4 ± 0.3 ns in ethylene glycol compared with 1.0 ± 0.1 ns in water. Second, the viscous solvent provides a cage for the methyl radical and introduces a geminate

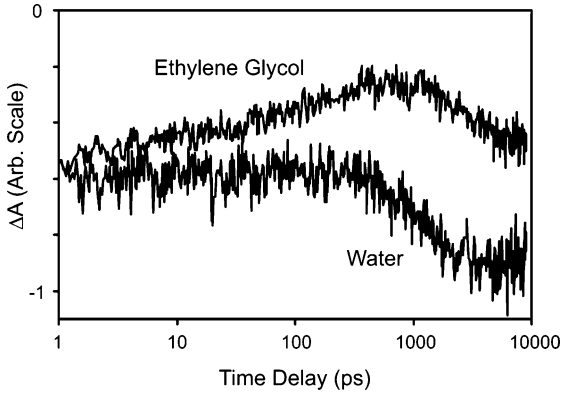

Figure 8. Comparison of the transient absorption signals at 520 nm for MeCbl in water and in ethylene glycol. The 175 ps decay of bleach observed in ethylene glycol has no equivalent signal in the data obtained in water.

recombination component clearly visible in the data. The 175 ps ($k_3 = 5.7$ ns^{-1}) decay associated spectrum (triangles) in Figure 7A has no analogue in the data obtained in water. The contrast between the behavior of MeCbl in water and ethylene glycol is illustrated more clearly in the time dependence of the spectral change at 520 nm, shown in Figure 8. The trace obtained in water is flat, with no change in absorption between a picosecond and a few hundred picoseconds, while the trace obtained in ethylene glycol exhibits a clear decay of the bleach. The wavelength-dependent amplitudes for this component reflect an overall decrease in the amplitude of the cob(II)alamin difference spectrum.

Assuming a model for the kinetic behavior of a system, species-associated difference spectra may be deduced from the decay-associated spectra. The simplest model consistent with the observations in MeCbl will have subpicosecond branching between prompt bond homolysis and formation of the MLCT excited state. The prompt bond homolysis is followed by recombination of the geminate radical pair and the formation of solvent-separated radical pairs. Formation of the MLCT state is followed by decay to either the ground electronic state or the radical pair. In water the branching between prompt homolysis and formation of the MLCT state was found to be 1:3.[25] Within the errors of the measurement, this same branching ratio is observed in ethylene glycol. Most of the population initially placed in the MLCT state ($\geq$85%) returns to the ground state without undergoing bond homolysis. However a small percentage may undergo bond cleavage, as observed for MeCbl in water following excitation at 520 nm.[25] The species-associated spectra deduced from this model are illustrated in Figure 7B. On the basis of the assumption that the spectra of the geminate radical pair and the solvent-separated radical pair will be identical, the quantum yield for cage escape, ϕ, is found to be 74% for methyl radical in ethylene glycol.

Discussion

Excited-State Lifetime and Photolysis Mechanism. In previous work on coenzyme B_{12} the observed photochemistry was found to be inherently sensitive to its environment, with very different excited-state progressions observed for AdoCbl in water, in ethylene glycol, and bound to glutamate mutase.[24,26−28] The influence of solvent environment on the excited electronic structure and the photochemistry of the simple alkylcobalamins MeCbl, EtCbl, and PrCbl investigated here is more subtle. The excited states and observed branching ratios are essentially identical in water and ethylene glycol. The dominant influence of the environment is found in the rates for formation of the solvent-separated radical pairs, in the decay of the MLCT excited state of MeCbl, and in the rate of relaxation observed for EtCbl and PrCbl. The insensitivity of the formation of the MLCT state to the solvent polarity suggests that the branching between bond homolysis and population of the long-lived excited state is a property of the initial vertical excitation and is not dependent upon the energy of the relaxed MLCT state. This conclusion is consistent with the insensitivity of the linear absorption spectrum and, by inference, the vertical excitation process to the solvent. It should be noted that the branching ratio is also unaffected by the binding of methylcobalamin in methionine synthase.[44]

While the formation of the MLCT state is unaffected by the environment, the decay of the MLCT state is influenced by the solvent. The lifetime of the excited state in ethylene glycol (2.4 ns) is more than a factor of 2 longer than the lifetime in water (1.0 ns). The influence of the solvent on the decay of the excited state may be attributed to several different mechanisms. Water and ethylene glycol are both polar, hydrogen-bonding solvents but are otherwise qualitatively and quantitatively different. Water is more polar than ethylene glycol (static dielectric constant 78.5 vs 37 at 25 °C),[29] has a much faster solvent reorientation time (0.34 ps vs 15 ps),[55] and has a lower shear viscosity (1 mPa s vs 19.9 mPa s at 20° C).[29]

There are three canonical modes of action for the influence of the solvent on the excited state lifetime. (1) The solvent environment may influence the decay of the excited state by modifying the energy of an intramolecular barrier for escape from the MLCT state. The polarity of the solvent will influence the barrier height if the reactant and the transition state have significantly different charge distributions. (2) The solvent friction may hinder any conformational motion of the cobalamin playing a role in a barrier crossing to the ground electronic state. According to Kramers theory for barrier crossing in the high friction limit, the rate constant should be inversely proportional to the coefficient of friction on the reaction coordinate, β.[56] In the simple hydrodynamic limit β will be proportional to the macroscopic shear viscosity, η. Clearly, this is not the case for the decay of the MLCT state. At 20 °C the shear viscosity of ethylene glycol is 20 times larger than that of water while the rate constant is only 2.4 times smaller. However, sublinear relationships between the friction on a reaction coordinate and the macroscopic shear viscosity are common.[56,57] (3) The solvent polarity may influence the stabilization of the MLCT state and modify the barrier height for return to the ground state. In addition solvent fluctuations and solvent reorganization may facilitate charge recombination and influence the relative rate constants for return to the ground state in water and ethylene glycol.

The viscosity and solvent dependence observed in methanol and ethylene glycol are consistent with any or all of these processes playing a role in the return to ground state. A more complete understanding of the process will require a better understanding of the electronic structure of cobalamins and data on the excited-state decay under a wider range of parameters.

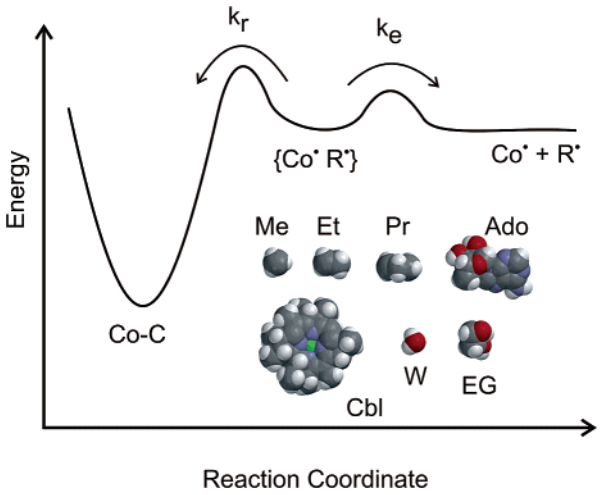

Figure 9. Schematic diagram of the competition between geminate recombination and cage escape. Space-filling models of the radical and solvent species are also shown for comparison of relative sizes. The species labeled Cbl is a model of the core corrin ring calculated with an imidazole lower axial ligand but without the phosphate link to the dimethylbenzimidazole and without the pendant groups around the periphery of the corrin ring.

Geminate Recombination of the Cob(II)•−R• Radical Pair. A schematic diagram sketching important features of geminate recombination in alkylcobalamins is shown in Figure 9. The solvent acts to cage the alkyl radical and inhibit the diffusive escape of the alkyl group. This change in the ability of the alkyl radical to escape the vicinity of the cob(II)alamin radical encourages geminate recombination and lowers the quantum yield for photolysis. Although diffusive recombination of a dilute radical pair is predicted to exhibit a complex dependence on time,[58] escape from the initial solvent cage can be modeled as an activated barrier crossing.[59,60]

Over the 9 ns time window of the experiments reported here, diffusive recombination is slow. Once the alkyl radical escapes the initial solvent cage, the dynamics are reasonably well approximated by an exponential decay to a long-lived radical pair. For the alkyl radical in the initial solvent cage, diffusion in any available direction represents cage escape and formation of a solvent separated radical pair. Once the first solvent-separated radical pair is formed, only backward diffusion, representing a small cone in all available space, will result in rapid recombination and the probability for recombination drops off. Competition between recombination and cage escape results in the initial exponential phase observed in the recombination of the radical pair. On a longer time scale, diffusive recombination will exhibit a much more complex time dependence.

Analysis of the data obtained for MeCbl, EtCbl, PrCbl, and AdoCbl demonstrate that the solvent environment has no significant impact on the rate constant for the recombination of the geminate radical pair. In the approximation that both recombination of the geminate radical pair and escape from the initial solvent cage obey first-order kinetics, the quantum yield for the formation of a long-lived radical pair is $\phi = k_e/(k_r + k_e)$. Both ϕ and $k_r + k_e$ are determined directly from the transient absorption data. The rate constant for the overall decay of the cob(II)alamin difference spectrum is the sum of the rate constants for recombination and escape, $k_r + k_e$. This sum is k_3 in MeCbl and k_4 in EtCbl and PrCbl. The quantum yield, ϕ, is determined from the relative amplitudes of the long-lived radical

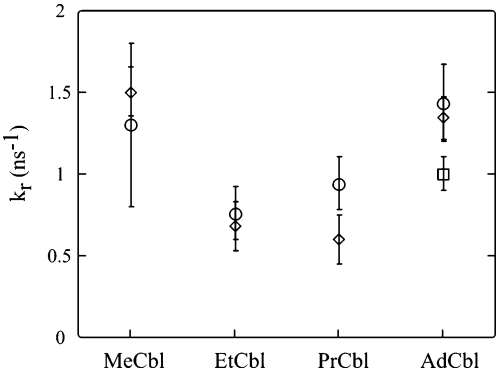

Figure 10. Rate constants for the geminate recombination of the alkyl radical with cob(II)alamin: circles, data obtained in water; diamonds, data obtained in ethylene glycol; square, data obtained for AdoCbl bound to glutamate mutase.

pair and the decay of the cob(II)alamin difference spectrum attributed to geminate recombination as described previously.[27] The rate constants for geminate recombination of MeCbl, EtCbl, PrCbl, and AdoCbl in water and ethylene glycol are compared in Figure 10. With the possible exception of PrCbl, intrinsic rate constants determined from the data obtained in water and in ethylene glycol are in good agreement with each other. For AdoCbl a uniform recombination rate constant was also determined in mixtures of water and ethylene glycol.[27] This lack of solvent dependence suggests that the activation barrier for recombination does not involve a conformational change of the corrin ring, where a solvent-dependent friction on the reaction coordinate would be expected. Rather, the lack of a solvent effect suggests that relaxation of the corrin ring to the alkylcobalamin geometry follows bond formation.

In contrast, the rate constant for geminate recombination of an alkylcobalamin is dependent upon the nature of the alkyl radical. The rate constants observed for the recombination of the biologically active coenzymes, MeCbl and AdoCbl, are approximately a factor of 2 larger than the rate constants for the recombination of EtCbl or PrCbl. As the cob(II)alamin cofactor is the same in all four recombination reactions, these data suggest that the rate constant for recombination is dependent upon geometric and/or electronic differences in the alkyl radicals. Electronic effects will modify the internal energy barrier for recombination, while geometric effects may introduce an additional entropic barrier to recombination. Dissociation of the alkyl radical will be followed by competing processes including diffusive reorientation or rotation of the alkyl radical within the initial solvent cage, translational diffusion of the alkyl radical out of the initial solvent cage, solvent reorientation to better solvate the radicals, and recombination of the radical pair.

Diffusive reorientation of the alkyl radical is a function of the volume of the radical, the shape of the radical (spherical, ellipsoidal, or irregular), and the friction of the surrounding solvent on the reorientation of the radical. In the hydrodynamic limit with stick boundary conditions the Stokes−Einstein−Debye expression for the rotational diffusion coefficient of a spherical object is

$$D_s = \frac{kT}{V\eta} \tag{2}$$

where k is the Boltzmann constant, T is the temperature, V is the volume of the solute, and η is the shear viscosity of the solvent. More complicated formulas, proportional to D_s, have been derived for rotation around the long and short axes of symmetric ellipsoids.[61]

Experimental measurements on small molecules, similar in size and shape to the radicals investigated here, may be used to estimate the anticipated reorientation times for these radicals. For example, the reorientation time of ammonium, a spherical cation slightly smaller than the methyl radical, ranges from 0.93 ps in water to 12.4 ps in ethylene glycol, a range qualitatively consistent with the anticipated $1/\eta$ dependence on viscosity.[62] On the other hand, the reorientation time of molecules comparable in size to the Ado radical are on the order of 70−140 ps/(mPa s) at room temperature.[63−70] Both water and ethylene glycol are protic, hydrogen-bonding solvents where the specific interactions between the Ado radical and the solvent will increase the effective hydrodynamic volume of the radical and slow the reorientation. Reorientation of the Et and Pr radicals will be slower than anticipated for Me but much faster than the reorientation of the Ado radical. It is reasonable to assume that reorientation of Me, Et, and Pr will range from values on the order of 1−3 ps in water to values on the order of 15−45 ps in ethylene glycol. Thus, reorientation of the small alkyl radicals is anticipated to be rapid with respect to the observed recombination rate, while reorientation of the Ado radical will be on a time scale comparable with (water) or slower than (ethylene glycol) the recombination.

The intrinsic recombination rate deduced from the data for MeCbl, EtCbl, and PrCbl will reflect recombination from a distribution of relative orientations. The difference in rate constants for the recombination of MeCbl, EtCbl, and PrCbl should reflect the influence of this distribution. The methyl radical recombination to form MeCbl will depend only weakly, if at all, on orientation, as recombination may occur from either side of the radical. The recombination of EtCbl and PrCbl, on the other hand, will depend on orientation, as recombination will only occur if the CH_2 end of the radical approaches the Cob(II)alamin. Rotational diffusion of the alkyl radical will add an entropic factor to the recombination and reduce the effective rate for geminate recombination over that expected for the properly oriented radical. This is qualitatively consistent with the ca. 1:2 ratio of the rate constants observed for recombination of MeCbl and EtCbl or PrCbl. AdoCbl falls in the opposite limit of slow reorientation, especially in ethylene glycol, and the observed recombination rate is comparable to that observed for MeCbl.

Influence of the Alkyl Radical on the Cage Effect. In the simple hydrodynamic model, the rate constant for cage escape is proportional to the translational diffusion coefficient of the solute radical in the solvent. Approximation of the translational diffusion coefficient generally begins with the well-known Stokes−Einstein equation:

$$D = \frac{kT}{6\pi r\eta} \tag{3}$$

This equation was derived for diffusion of a spherical particle through a continuous medium and is a reasonable approximation for a large solute dissolved in a solvent composed of small molecules. The factor of 6π in the denominator of eq 3 assumes stick boundary conditions, while a factor of 4 π is derived for slip boundary conditions. These expressions may be generalized to describe the diffusion of ellipsoidal molecules. For a spherical particle in a solvent of comparable size, the factor in the denominator is replaced by $\alpha\pi r\eta$, where α is a variable factor determined by the effective length of the path taken by the solvent to exchange places with the solute. In the context of the present investigation, the diffusion of the cob(II)alamin radical will be effectively zero and the cage escape will reflect

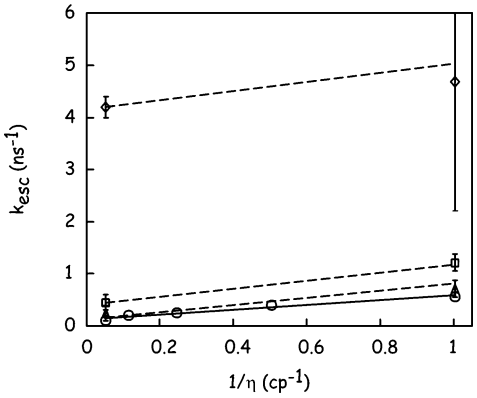

Figure 11. Rate constants for "cage escape" as a function of $1/\eta$, where η is the solvent shear viscosity (1 cp = 10^{-3} Pa s = 1 mPa s): circles, AdoCb; triangles, PrCbl; squares, EtCbl; diamonds, MeCbl. Error bars are derived from the ability to determine quantum yields from the data. The error bars for the AdoCbl data are no larger than the circles as drawn. The solid line is a least-squares fit to the AdoCbl data. The dashed lines have the slopes predicted by the Stokes−Einstein equation for diffusion of the other akyl radicals but are offset by a variable "infinite viscosity" intercept.

TABLE 2: Summary of Solvent Dependence of Cage Escape for MeCbl, EtCbl, PrCbl, and AdoCbl ($k_{esc} = m/\eta + b$; m = 0.46 (r_{Ado}/r_R)

	R•			
param	Me	Et	Pr	Ado
r_R (Å)	2.0	2.3	2.5	3.8
m (ns^{-1} cp^{-1})	0.89	0.76	0.69	0.46
b (ns^{-1})	4	0.4	0.2	0.13

only the diffusion of the alkyl radical R• to form the initial solvent separated radical pair.

In the limit where eq 3 is approximately valid, the rate constant for cage escape by radicals of differing size should be inversely proportional to the viscosity of the solvent and inversely proportional to the size of the radical R•. The principle consequence of the dependence on size is a change in the slope of a plot of k_e vs $1/\eta$. In agreement with this expectation, the diffusion coefficients measured for methane, ethane, propane, and *n*-butane in water exhibit a size dependence consistent with the factor α weakly dependent on the size of the radical.[71]

The rate constants for the cage escape of methyl, ethyl, *n*-propyl, and 5′-deoxyadenosyl radicals in water and ethylene glycol are plotted vs $1/\eta$ in Figure 11. The solid line is the fit of the AdoCbl data for geminate recombination in water, ethylene glycol, and mixtures of water and ethylene glycol. These data exhibit a linear dependence with $k_{esc} = 0.46$ ns^{-1} $cp^{-1} \pm 0.07$ ns^{-1} $cp^{-1}/\eta + 0.13$ $ns^{-1} \pm 0.04$ ns^{-1}.[27] The dashed lines represent fits of data obtained for the other alkylcobalamins to a line with a slope determined by the expected influence of radical size on the slope: $m_R = 0.46$ ns^{-1} cp^{-1} (r_{Ado}/r_R). The intercept is allowed to vary freely. The parameters are summarized in Table 2. The radius of each radical was estimated by calculating the equilibrium geometry and volume of the radical (6−31G** calculation in Spartan04) and assuming that the radical is approximately spherical. Clearly this is a rough approximation, but the available data do not warrant a more complex analysis. The viscosity dependence of the rate constant for cage escape is consistent with the anticipated trend.

The intercept for each radical in Figure 11 describes the viscosity-independent formation of a radical pair with a lifetime much longer than the 9 ns window of observation available in the present measurements. The rate constant for the formation of the long-lived radical correlates with the size of the radical, does not appear to depend strongly on the solvent, and is not due to diffusion-controlled escape from the initial solvent cage. In the earlier interpretation of the data for AdoCbl, it was suggested that this intercept reflects either a conformational change in the Ado radical or the cob(II)alamin, a rotation of the Ado radical, or the evolution from a singlet radical pair to a triplet radical pair.[27] The latter mechanism was favored and may dominate for the larger radicals. However, the evolution between singlet and triplet radical pairs will not account for the very rapid formation of a long-lived radical pair following excitation of MeCbl.

The anomalous rapid formation of a long-lived methyl radical following excitation of MeCbl may reflect the influence of the photolysis mechanism. The cob(II)alamin species observed following excitation of MeCbl at 400 nm is formed promptly on a subpicosecond time scale, suggesting excitation to a directly dissociative excited state. In this limit the methyl radical will be formed with an excess translational kinetic energy, not in equilibrium with the surroundings. This initial excess energy may enhance cage escape and increase the yield of solvent-separated radical pairs. In contrast AdoCbl dissociates on a time scale of tens of picoseconds with several distinct intermediate states observed prior to formation of the steady-state cob(II)-alamin spectrum. In this system the Ado radical will be formed at or near thermal equilibrium with the surroundings.

Excitation of EtCbl or PrCbl at 400 nm appears to access a directly dissociative excited state, although the evidence is not as clear as for MeCbl. However, the 100 ps relaxation of the corrin ring suggests that the energy partitioning is different in EtCbl and PrCbl than in MeCbl. In addition the radicals are two or three times more massive, a factor of 1.5−2 times larger, they will move somewhat more slowly, and will not move through holes in the surrounding solvent with as much ease. As a result, these systems may be expected to thermalize much more quickly. The decrease in the intercept with the increasing size of the radical is consistent with this expectation.

Summary and Conclusions

In this paper we have extended our studies of the photolysis of alkylcobalamins to explore the effect of the solvent environment, ethylene glycol vs water. Measurements of the excited-state dynamics and geminate recombination of MeCbl, EtCbl, and PrCbl were carried out and compared with the results reported earlier for AdoCbl. These measurements probe three different aspects of the influence of solvent.

(1) These experiments probe the formation and decay of the MLCT intermediate observed following excitation of MeCbl. Excitation of MeCbl in ethylene glycol at 400 nm leads to a branching between prompt dissociation and formation of this MLCT excited state as observed in aqueous solution. The branching ratio is 3:1 MLCT formation vs prompt homolysis. This ratio is unaffected by the solvent. On the other hand, the solvent modifies the rate constant for the decay of the MLCT excited state, increasing the lifetime of this state from 1 ns in water to 2.4 ns in ethylene glycol. This suggests an influence of the solvent on the decay through the electrostatic influence of the solvent polarity on the barrier for decay or through the influence of solvent friction on the reaction.

(2) These experiments probe the intrinsic geminate recombination of the cob(II)alamin with the alkyl radical. The recombination rate constant is at most weakly dependent on the solvent. There is no measurable variation in the recombination rates of Me, Et, and Ado radicals. The recombination of

Pr with cob(III)alamin in ethylene glycol is no more than 30% slower than the rate constant observed in water. These results suggest that the activation barrier for recombination does not involve a conformational change of the corrin ring, where a solvent-dependent friction on the reaction coordinate would be expected. The rate constants observed for the recombination of Et and Pr radicals with cob(II)alamin are a factor of 2 slower than the rate constants for the recombination of Me and Ado with cob(II)alamin. This difference is consistent with reorientation of the alkyl radicals and the anticipated dependence of the recombination process on the geometry of approach.

(3) These experiments help elucidate the role of the solvent cage in promoting recombination of the geminate radical pair. The Et, Pr, and Ado radicals are produced in a state near thermal equilibrium with the surroundings or rapidly approach thermal equilibrium with the surroundings. These radicals exhibit the behavior expected for diffusion-controlled escape from the initial solvent cage. The cage effect following photodissociation of these species may be reasonably used as a model for thermolysis. In contrast the methyl radical is produced by prompt bond dissociation and the magnitude of cage escape is much larger than anticipated on the basis of hydrodynamic arguments and the size of the radical. The high quantum yield for cage escape in MeCbl reflects the photolysis mechanism and the dissipation of the excess energy deposited by the excitation photon. This suggests that photodissociation and recombination of MeCbl is not a good model system for the related thermal bond homolysis.

Acknowledgment. This work was supported by the NSF (Grant CHE 0078972) and the NIH (Grant DK53842).

References and Notes

(1) Marsh, E. N. G. *Essays Biochem.* **1999**, *34*, 139−154.
(2) Marsh, E. N. G.; Drennan, C. L. *Curr. Opin. Chem. Biol.* **2001**, *5*, 499−505.
(3) Banerjee, R. *Chem. Biol.* **1997**, *4*, 175−186.
(4) Banerjee, R. *Biochemistry* **2001**, *40*, 6191−6198.
(5) Banerjee, R. *Chem. Rev.* **2003**, *103*, 2083−2094.
(6) Banerjee, R.; Matthews, R. G. *FASEB J.* **1990**, *4*, 1450−1459.
(7) Ludwig, M. L.; Matthews, R. G. *Annu. Rev. Biochem.* **1997**, *66*, 269−313.
(8) Harms, U.; Thauer, R. K. *Eur. J. Biochem.* **1996**, *241*, 149−154.
(9) Paul, L.; Krzycki, J. A. *J. Bacteriol.* **1996**, *178*, 6599−6607.
(10) Seravalli, J.; Brown, K. L.; Ragsdale, S. W. *J. Am. Chem. Soc.* **2001**, *123*, 1786−1787.
(11) Banerjee, R., Ed. *Chemistry and biochemistry of B_{12}*; Wiley: New York, 1999; p 921.
(12) Andruniow, T.; Kozlowski, P. M.; Zgierski, M. Z. *J. Chem. Phys.* **2001**, *115*, 7522−7533.
(13) Andruniow, T.; Zgierski, M. Z.; Kozlowski, P. M. *J. Phys. Chem. B* **2000**, *104*, 10921−10927.
(14) Andruniow, T.; Zgierski, M. Z.; Kozlowski, P. M. *Chem. Phys. Lett.* **2000**, *331*, 502−508.
(15) Andruniow, T.; Zgierski, M. Z.; Kozlowski, P. M. *Chem. Phys. Lett.* **2000**, *331*, 509−512.
(16) Andruniow, T.; Zgierski, M. Z.; Kozlowski, P. M. *J. Am. Chem. Soc.* **2001**, *123*, 2679−2680.
(17) Andruniow, T.; Zgierski, M. Z.; Kozlowski, P. M. *J. Phys. Chem. A* **2002**, *106*, 1365−1373.
(18) Brooks, A. J.; Vlasie, M.; Banerjee, R.; Brunold, T. C. *J. Am. Chem. Soc.* **2004**, *126*, 8167−8180.
(19) Stich, T. A.; Brooks, A. J.; Buan, N. R.; Brunold, T. C. *J. Am. Chem. Soc.* **2003**, *125*, 5897−5914.
(20) Stich, T. A.; Buan, N. R.; Brunold, T. C. *J. Am. Chem. Soc.* **2004**, *126*, 9735−9749.
(21) Randaccio, L.; Geremia, S.; Stener, M.; Toffoli, D.; Zangrando, E. *Eur. J. Inorg. Chem.* **2002**, 93−103.
(22) Ouyang, L.; Randaccio, L.; Rulis, P.; Kurmaev, E. Z.; Moewes, A.; Ching, W. Y. *J. Mol. Struct.: THEOCHEM* **2003**, *622*, 221−227.
(23) Kozlowski, P. M.; Zgierski, M. Z. *J. Phys. Chem. B* **2004**, *108*, 14163−14170.
(24) Sension, R. J.; Cole, A. G.; Harris, A. D.; Fox, C. C.; Woodbury, N. W.; Lin, S.; Marsh, E. N. G. *J. Am. Chem. Soc.* **2004**, *126*, 1598−1599.
(25) Shiang, J. J.; Walker, L. A., II; Anderson, N. A.; Cole, A. G.; Sension, R. J. *J. Phys. Chem. B* **1999**, *103*, 10532−10539.
(26) Walker II, L. A.; Shiang, J. J.; Anderson, N. A.; Pullen, S. H.; Sension, R. J. *J. Am. Chem. Soc.* **1998**, *120*, 7286−7292.
(27) Yoder, L. M.; Cole, A. G.; Walker, L. A., II; Sension, R. J. *J. Phys. Chem. B* **2001**, *105*, 12180−12188.
(28) Sension, R. J.; Harris, D. A.; Stickrath, A.; Cole, A. G.; Fox, C. C.; Marsh, E. N. G. *J. Phys. Chem. B* **2005**, *109*, 18146−18152.
(29) Weast, R. C., Ed. *Handbook of Chemistry and Physics*, 62nd ed.; CRC Press: Boca Raton, FL, 1982.
(30) Noyes, R. M. *J. Chem. Phys.* **1954**, *22*, 1349−1359.
(31) Lampe, F. W.; Noyes, R. M. *J. Am. Chem. Soc.* **1954**, *76*, 2140−2144.
(32) Noyes, R. M. *J. Am. Chem. Soc.* **1955**, *77*, 2042−2045.
(33) Noyes, R. M. *Annu. Rev. Phys. Chem.* **1956**, *7*, 185−206.
(34) Noyes, R. M. *J. Am. Chem. Soc.* **1956**, *78*, 5486−5490.
(35) Koenig, T. W.; Finke, R. G. *J. Am. Chem. Soc.* **1988**, *110*, 2657−2658.
(36) Koenig, T. W.; Hay, B. P.; Finke, R. G. *Polyhedron* **1988**, *7*, 1499−1516.
(37) Gerards, L. E. H.; Bulthuis, H.; Bolster, M. W. G. d.; Balt, S. *Inorg. Chim. Acta* **1991 19***0*, 47−53.
(38) Chen, E.; Chance, M. R. *J. Biol. Chem.* **1990**, *265*, 12987−12994.
(39) Lott, W. B.; Chagovetz, A. M.; Grissom, C. B. *J. Am. Chem. Soc.* **1995**, *117*, 12194−12201.
(40) Chagovetz, A. M.; Grissom, C. B. *J. Am. Chem. Soc.* **1993**, *115*, 12152−12157.
(41) Endicott, J. F.; Netzel, T. L. *J. Am. Chem. Soc.* **1979**, *101*, 4000−4002.
(42) Cole, A. G.; Yoder, L. M.; Shiang, J. J.; Anderson, N. A.; Walker, L. A., II; Banaszak Holl, M. M.; Sension, R. J. *J. Am. Chem. Soc.* **2002**, *124*, 434−441.
(43) Wilhelm, T.; Piel, J.; Riedle, E. *Opt. Lett.* **1997**, *22*, 1494−1496.
(44) Walker, L. A., II; Jarrett, J. T.; Anderson, N. A.; Pullen, S. H.; Matthews, R. G.; Sension, R. J. *J. Am. Chem. Soc.* **1998**, *120*, 3597−3603.
(45) Dong, S.; Padmakumar, R.; Banerjee, R.; Spiro, T. G. *J. Am. Chem. Soc.* **1996**, *118*, 9182−9183.
(46) Dong, S.; Padmakumar, R.; Banerjee, R.; Spiro, T. G. *Inorg. Chim. Acta* **1998**, *270*, 392−398.
(47) Dong, S.; Padmakumar, R.; Maiti, N.; Banerjee, R.; Spiro, T. G. *J. Am. Chem. Soc.* **1998**, *120*, 9947−9948.
(48) Dong, S.; Padmakumar, R.; Banerjee, R.; Spiro, T. G. *J. Am. Chem. Soc.* **1999**, *121*, 7063−7070.
(49) Huhta, M. S.; Chen, H.-P.; Hemann, C.; Hille, C. R.; Marsh, E. N. G. *Biochem. J.* **2001**, *355*, 131−137.
(50) Mayer, E.; Gardiner, D. J.; Hester, R. E. *Biochim. Biophys. Acta* **1973**, *297*, 568−570.
(51) Thomson, A. J. *J. Am. Chem. Soc.* **1969**, *91*, 2780−&.
(52) Fugate, R. D.; Chin, C.-A.; Song, P.-S. *Biochim. Biophys. Acta* **1976**, *421*, 1−11.
(53) Jaworska, M.; Lodowski, P. *J. Mol. Struct.: THEOCHEM* **2003**, *631*, 209−223.
(54) Day, P. *Coord. Chem. Rev.* **1967**, *2*, 99−108.
(55) Maroncelli, M. *J. Chem. Phys.* **1997**, *106*, 1545−1555.
(56) Hanggi, P.; Talkner, P.; Borkovec, M. *Rev. Mod. Phys.* **1990**, *62*, 251−341.
(57) Anderson, N. A.; Pullen, S. H.; Walker II, L. A.; Shiang, J. J.; Sension, R. J. *J. Phys. Chem. A* **1998**, *102*, 10588−10598.
(58) Hynes, J. T. *Annu. Rev. Phys. Chem.* **1985**, *36*, 573−597.
(59) Hirschfelder, J.; Stevenson, D.; Eyring, H. *J. Chem. Phys.* **1937**, *5*, 896−912.
(60) Eyring, H. *J. Chem. Phys.* **1936**, *4*, 283−291.
(61) Perrin, F. *J. Phys. Radium* **1934**, *5*, 497.
(62) Masuda, Y. *J. Phys. Chem. A* **2001**, *105*, 2989−2996.
(63) Dutt, G. B. *J. Chem. Phys.* **2000**, *113*, 11154−11158.
(64) Dutt, G. B.; Ghanty, T. K. *J. Chem. Phys.* **2003**, *118*, 4127−4133.
(65) Dutt, G. B.; Krishna, G. R. *J. Chem. Phys.* **2000**, *112*, 4676−4682.
(66) Dutt, G. B.; Krishna, G. R.; Raman, S. *J. Chem. Phys.* **2001**, *115*, 4732−4741.
(67) Dutt, G. B.; Raman, S. *J. Chem. Phys.* **2001**, *114*, 6702−6713.
(68) Dutt, G. B.; Srivatsavoy, V. J. P.; Sapre, A. V. *J. Chem. Phys.* **1999**, *111*, 9705−9710.
(69) Moog, R. S.; Ediger, M. D.; Boxer, S. G.; Fayer, M. D. *J. Phys. Chem.* **1982**, *86*, 4694−4700.
(70) Rice, S. A.; Kenney-Wallace, G. A. *Chem. Phys.* **1980**, *47*, 161−170.
(71) Witherspoon, P. A.; Saraf, D. N. *J. Phys. Chem.* **1965**, *69*, 3752−3755.